Preprints.org

Article

Not peer-reviewed version

Preparation, Characterization, and Antibiofilm Effect of Free and Nanoencapsulated *Tetradenia riparia* (Hochst) Codd Leaves Essential Oil

Regina Yasuko Makimori , Eliana Harue Endo , Julia Watanabe Makimori , Priscila Firmino Ribas , Fernanda Vitória Leimann , Odinei Hess Gonçalves , Zilda Cristiani Gazim , Tânia Ueda-Nakamura , Celso Vataru Nakamuira , Benedito Prado Dias Filho *

Posted Date: 5 December 2025

doi: 10.20944/preprints202512.0548.v1

Keywords: myrrh; *Staphylococcus aureus*; biofilm; essential oil; nanoparticle

Preprints.org is a free multidisciplinary platform providing preprint service that is dedicated to making early versions of research outputs permanently available and citable. Preprints posted at Preprints.org appear in Web of Science, Crossref, Google Scholar, Scilit, Europe PMC.

Copyright: This open access article is published under a Creative Commons CC BY 4.0 license, which permit the free download, distribution, and reuse, provided that the author and preprint are cited in any reuse.

Preprints.org (www.preprints.org) | NOT PEER-REVIEWED | Posted: 5 December 2025 doi:10.20944/preprints202512.0548.v1

Disclaimer/Publisher's Note: The statements, opinions, and data contained in all publications are solely those of the individual author(s) and contributor(s) and not of MDPI and/or the editor(s). MDPI and/or the editor(s) disclaim responsibility for any injury to people or property resulting from any ideas, methods, instructions, or products referred to in the content.

Article

Preparation, Characterization, and Antibiofilm Effect of Free and Nanoencapsulated *Tetradenia riparia* (Hochst) Codd Leaves Essential Oil

Regina Yasuko Makimori [1], Eliana Harue Endo [1], Julia Watanabe Makimori [1], Priscila Firmino Ribas [1], Fernanda Vitória Leimann [2], Odinei Hess Gonçalves [2], Zilda Cristiani Gazim [3], Tânia Ueda-Nakamura [1], Celso Vataru Nakamura [1] and Benedito Prado Dias Filho [1,*]

[1] Postgraduate Program in Pharmaceutical Sciences, State University of Maringá, PR, Brazil
[2] Food Department, Federal Technological University of Campo Mourão, Campo Mourão, PR, Brazil
[3] Postgraduate Program in Biotechnology Applied to the Agriculture and Postgraduate Program in Animal Science with Emphasis on Bioactive Products, Paranaense University, PR, Brazil
* Correspondence: bpdfilho@uem.br. Av. Colombo, 5790. Maringá, PR, Brazil. Phone number: +55 44 3011-5049

Abstract

Staphylococcus aureus is an important microorganism that has the ability to form biofilm on a various range of surfaces. Factors contributing to the reduction of the effectiveness of the treatment are the development of resistance to antimicrobial drugs. Essential oils (EO) are effective and economical alternatives, however with the disadvantage of rapid oxidation, nanoencapsulation is an alternative that improves stability, reduces toxicity and controls the release of oil. Nanoprecipitation with Poly-lactide was used to obtain nanoparticles (NP) with EO. The antibiofilm effect was observed by the broth microdilution method. A cytotoxic assay was performed using a VERO cell line. Nanoparticles were found to be nanometric, round with regular structures. EO and NP show antibacterial and antibiofilm activity against *S. aureus*. NP was less cytotoxic than EO.aure Nanoparticle prevented rapid EO evaporation and degradation and enhanced its stability. NP stability was studied using zeta potential. Its value was determined to be around -23.1 mV, which indicates that NP are in fact stable. Melting temperature and melting enthalpy for Blank NP were 54.29 °C and 429.63 J/g. The decreasing in melting enthalpy from 429.63 to 115.83 J/g in NP containing EO makes this system favorable to controlled release of essential oils. NP has a smaller area under the peak, indicating that the EO may modify the crystalline organization, facilitating melting and thus the release of EO. EO and NP presented a growth inhibition of planktonic and biofilm formation against *S. aureus*. NP were less cytotoxic than free EO. Thus, these findings may contribute to the development of new strategies against infections caused by *S. aureus*.

Keywords: myrrh; *Staphylococcus aureus*; biofilm; essential oil; nanoparticles

---

1. Introduction

Staphylococcus aureus is a Gram-positive and aerophilic bacterium responsible for the most common skin infections, including dermatitis. The pathogen colonizes more than 20% of the population asymptomatically but can cause symptomatic infections when the epithelial barrier is compromised [1]. Planktonic *S. aureus* can adhere to surfaces, proliferate, produce extracellular matrix, and ultimately form biofilms. Once mature, biofilms release individual cells or fragments that can colonize new surfaces. Biofilms account for approximately 80% of microbial infections and exhibit up to 1000-fold greater resistance and tolerance to antibiotics compared with planktonic cells [2,3].

© 2025 by the author(s). Distributed under a Creative Commons CC BY license.

Preprints.org (www.preprints.org) | NOT PEER-REVIEWED | Posted: 5 December 2025 doi:10.20944/preprints202512.0548.v1

Conventional antibacterial agents present several limitations, including adverse side effects, poor solubility, drug–drug interactions, induction of antimicrobial resistance, and reduced efficacy [4]. Consequently, there is increasing interest in developing safer and more effective antibacterial alternatives. Aromatic plants and their essential oils (EOs) have long been used in traditional medicine and demonstrate broad antimicrobial properties [5]. Essential oils are complex mixtures of volatile compounds, predominantly monoterpenes, sesquiterpenes, and phenylpropanoids, with terpenes primarily responsible for their biological activity [6]. Their antimicrobial effect arises mainly from their high hydrophobicity and abundance of short-chain carbon compounds (particularly terpenes), which interact strongly with membrane lipids, altering membrane fluidity and integrity. This disruption ultimately leads to pathogen death [7].

Tetradenia riparia (Hochst.) Codd, a member of the *Lamiaceae* family, is an herbaceous shrub 1–3 m tall, widely distributed across Africa. It is commonly known as false myrrh, lemon verbena, lavandula, misty plume, or incense [8,9]. The species has been traditionally used to treat cough, edema, diarrhea, fever, headache, malaria, and toothache. Its essential oil exhibits larvicidal, insecticidal, antimalarial, antimicrobial, and antinociceptive activities. The oil contains a complex mixture of monoterpenes, diterpenes, and sesquiterpenes, with calyculone, caryophyllene, β,13β-epoxy-7-abietene, fenchone, terpineol, 14-hydroxy-9-caryophyllene, and germacrene-D-4-ol identified as major constituents responsible for its biocidal properties [10–12].

Despite their strong antimicrobial potential, essential oils are prone to volatilization, degradation, and loss of activity upon exposure to light, heat, or pressure. Nanoencapsulation of EOs into polymeric nanoparticles helps preserve their functional properties, enhance stability, control release, reduce toxicity, and improve water solubility [7,13]. Therefore, the aim of this study was to prepare polymeric nanoparticles containing *T. riparia* essential oil using nanoprecipitation, characterize their physicochemical properties, and evaluate their cytotoxicity and antibiofilm activity against *S. aureus*.

2. Materials and Methods

2.1. Plant Material, Botanical Identification, and Extraction of Essential Oils

Fresh *Tetradenia riparia* leaves were collected in western Paraná State, Brazil, in December 2015. The plant was identified by Professor Ezilda Jacomasi, Department of Pharmacy, Paranaense University (UNIPAR), Paraná. A voucher specimen was deposited in the UNIPAR Herbarium (code 2502).

The essential oil (EO) was extracted by hydrodistillation for 3 h using a modified Clevenger-type apparatus, according to the procedure described in reference [14]. The distilled EO was collected, dried over anhydrous Na_2SO_4, and stored in amber glass flasks at −4 °C until use, following the method described in [15].

2.2. Chemical Identification of Essential Oils

The chemical compositions of *T. riparia* EO before and after storage were determined by gas chromatography–mass spectrometry (GC–MS). Compounds were identified by comparing their Kovats retention indices with those of known substances and by comparison with mass spectra from reference databases. Relative quantities (%) were calculated directly from GC peak areas.

GC–MS analyses were performed using a Focus GC system (Thermo Electron Corporation) equipped with a DBS-MS column (30 m × 0.25 mm × 0.25 µm). The injector and transfer line temperatures were set at 230 °C. The oven temperature program was as follows: initial temperature 60 °C for 1 min, then increased at 3 °C/min to 220 °C and held for 5 min. Hydrogen was used as the carrier gas. The injection volume was 5 µL (split 1:10), and the ionization energy was 70 eV. Mass spectra were obtained at 230 °C using a DSQ II detector (Thermo Scientific) in total ion current (TIC) acquisition mode, with a mass range of 50–659 m/z.

© 2025 by the author(s). Distributed under a Creative Commons CC BY license.

Preprints.org (www.preprints.org) | NOT PEER-REVIEWED | Posted: 5 December 2025

doi:10.20944/preprints202512.0548.v1

2.3. Nanoparticle Preparation

Poly(L-lactide) nanoparticles (NP) were prepared by the nanoprecipitation method using the dropping technique. The organic phase, consisting of 50 mg EO and 50 mg PLA (MW 90,000–120,000; Sigma-Aldrich) in 4 mL acetone, was added dropwise into the aqueous phase (10 mL of 1.0% w/v Pluronic F68; Sigma-Aldrich) under stirring at 1200 rpm for 30 min. Acetone was removed using a rotary evaporator. Blank PLA nanoparticles (without EO) were prepared using the same procedure. The final NP suspension was stored at 4 °C until further analysis.

2.4. Nanoparticle Characterization

Particle size and distribution were measured by dynamic light scattering (DLS) using a NanoPlus zeta/nanoparticle analyzer. Samples were diluted in ultrapure water prior to analysis.

Surface morphology was examined using a Shimadzu SS-550 scanning electron microscope (SEM). Samples of the nanosuspension were placed on glass plates, dried under reduced pressure at 25 °C, coated with gold using a sputter coater, and examined by SEM.

Transmission electron microscopy (TEM) was used to further evaluate morphology and size distribution. Samples were deposited onto copper grids, stained with 1% w/v uranyl acetate for 1 min, dried, and analyzed by TEM.

2.5. Thermal Analysis

Thermal properties of blank NP and EO-loaded NP were determined by differential scanning calorimetry (DSC; PerkinElmer DSC4000). Samples (3–5 mg) were placed in aluminum pans and heated from 20 to 200 °C at 20 °C/min under nitrogen flow (50 mL/min).

2.6. Encapsulation Efficiency

The EO content of NP was quantified by UV–visible spectroscopy (Shimadzu UV–VIS). A standard curve was prepared by serial dilution of EO in absolute ethanol and measuring absorbance at 325 nm [14].

For EO quantification in NP, 2 mg of sample was dissolved in 2 mL absolute ethanol, and absorbance at 325 nm was compared to the standard curve. Encapsulation efficiency was calculated as:

$$\%EE = (\text{total loaded EO} / \text{initial EO}) \times 100.$$

2.7. In Vitro Release Profile

Ten milligrams of NP or EO were placed in individual dialysis bags containing 40 mL PBS and incubated on a shaker at 37 °C. A 2 mL aliquot of the release medium was collected at 0, 15, 30, 60, 90, 120, and 360 min, and replaced with fresh PBS. EO release was quantified by UV–visible spectroscopy at 325 nm [16].

2.8. Stability Assays

A stability assay was conducted over 30–45 days at 25 ± 2 °C according to RDC 45 (August 9, 2012) [17]. The antibacterial activity of *T. riparia* EO and NP was subsequently analyzed using the broth microdilution assay following CLSI guidelines.

2.9. Strains and Growth Conditions

Staphylococcus aureus ATCC 29213 was used as the test strain. The bacterium was maintained on Mueller–Hinton agar (MHA; Difco) at 4 °C and cultured in Mueller–Hinton broth (MHB; Difco) before assays.

© 2025 by the author(s). Distributed under a Creative Commons CC BY license.

Preprints.org (www.preprints.org) | NOT PEER-REVIEWED | Posted: 5 December 2025 doi:10.20944/preprints202512.0548.v1

2.10. Microdilution Assay

Antibacterial activity was assessed by broth microdilution following CLSI guidelines [17]. Serial two-fold dilutions of EO and NP were prepared in 96-well plates containing 100 µL sterile MHB. Bacterial inoculum (10^5 CFU/mL) was added to each well. Plates were incubated at 37 °C for 24 h.

The minimum inhibitory concentration (MIC) was defined as the lowest concentration preventing visible growth. Minimum bactericidal concentration (MBC) was determined by subculturing 10 µL from wells with no visible growth onto MHA plates, followed by incubation at 37 °C for 24 h.

2.11. Antibiofilm Activity

A 100 µL bacterial suspension (1×10^8 CFU/mL) prepared in tryptic soy broth (TSB) supplemented with 1% glucose was added to wells containing EO or NP dilutions and incubated at 37 °C for 24 h. Wells were washed with PBS.

For the MTT assay, 20 µL MTT solution (2 mg/mL in PBS) was added, and plates were incubated for 2 h at 37 °C. After removing the MTT solution, 100 µL DMSO was added to solubilize formazan crystals. Absorbance was measured at 570 nm [18].

The biofilm inhibitory concentration (BIC_{50}) was defined as the minimum concentration that inhibited ≥50% of biofilm viability relative to untreated controls.

2.12. Cytotoxicity Assay

Cytotoxicity of EO and NP was evaluated using an MTT assay according to Tangarife-Castaño et al. [19]. VERO cells (African green monkey kidney; Cercopithecus aethiops) were cultured in DMEM for 72 h. Cell monolayers were trypsinized, washed, and seeded at 2.5×10^5 cells/well in 96-well plates.

After 24 h, EO and NP (1, 10, 100, and 1000 µg/mL) were added to wells, followed by incubation for 72 h at 37 °C in 5% CO_2. Cells were washed with PBS and incubated with 2 mg/mL MTT for 4 h. Formazan crystals were solubilized with 200 µL DMSO, and absorbance was measured at 530 nm using a Biotek PowerWave XS reader.

The IC_{50} values were obtained by linear regression of dose–response curves generated in R software. Selectivity indices (SI) were calculated as SI = IC_{50} / MIC.

3. Results and Discussion

3.1. Chemical Composition of Tetradenia riparia Leaf Essential Oil

The antimicrobial activity of essential oils (EOs) depends on their chemical composition. The major compounds present in *Tetradenia riparia* EO were identified by GC–MS. The EO yield was 0.33% of plant material. The composition and yield of essential oils are known to be affected by seasonal variations [10]. Previous studies reported the highest EO yield from *T. riparia* leaves in winter (0.265%). In contrast, EO content decreased to 0.168% during spring, likely due to the substantially higher rainfall observed in this season.

Table 1 lists the compounds identified in the EO prior to nanoencapsulation (free EO). The major chemical classes were oxygenated monoterpenes (28.94%), with fenchone (27.19%) as the predominant constituent, and oxygenated sesquiterpenes (34.30%), mainly represented by α-cadinol (16.12%) and 14-hydroxy-9-epi-caryophyllene (13.09%) (Figure S1 supplementary data). Hydrocarbon sesquiterpenes (11.7%) were also noteworthy, particularly due to the presence of caryophyllene (8.40%). These results agree with the chemical characterization reported for *T. riparia* leaf EO by Gazim et al. [10].

© 2025 by the author(s). Distributed under a Creative Commons CC BY license.

Preprints.org (www.preprints.org) | NOT PEER-REVIEWED | Posted: 5 December 2025
doi:10.20944/preprints202512.0548.v1

Table 1. CG-MS analysis of *T. riparia* leaves essential oil.

Peak	R.T. (min)	Compounds	Relative area %	RI Calc.	RI Lit.	Literature
1	3.6	α-pinene	1.25	906	910	20
2	4.4	Camphene	0.97	951	952	21
3	5.5	Fenchone	27.19	1091	1092	22
4	6	Fenchol	0.41	1116	1117	23
5	6.7	Camphor	1.02	1148	1149	24
6	7.2	endo-Borneol	0.19	1168	1168	25
7	7.8	Terpinen-4-ol	0.13	1180	1181	26
8	11.7	alfa-copaene	0.18	1375	1376	27
9	12.8	β-elemene	0.18	1390	1390	28
10	13.3	α-gurjunene	0.18	1408	1408	27
11	14.2	Caryophyllene	8.4	1418	1418	29
12	14.6	γ-Elemene	1.88	1427	1425	30
13	15.3	γ-muurolene	0.88	1475	1475	31
14	16.4	6-*epi*-shyobunol	1.08	1522	1522	32
15	17.1	Germacrene D-4-ol	1.06	1574	1574	28
16	17.8	(-)-Spathulenol	0.12	1576	1576	33
17	18.6	Caryophyllene oxide	1.02	1581	1581	34
18	19.4	Ledol	0.18	1605	1607	35
19	20.7	δ-cadinol	1.63	1649	1649	36
20	21.2	α-cadinol	16.12	1668	1674	37
21	21.9	14-hydroxy-9-epi-caryophyllene	13.09	1690	1674	34
22	29.2	9β,13β-Epoxi-7-abietene	11.5	1883	1888	38
23	31.1	Abietadiene	0.98	2081	2085	38
24	33.6	6,7-dehydroroyleanone	8.73	2094	2094	38
		Total identified	98.37			
		Hydrocarbon monoterpenes	2.22			
		Oxygenated monoterpenes	28.94			
		Hydrocarbon sesquiterpenes	11.7			
		Oxygenated sesquiterpenes	34.3			
		Diterpenes hydrocarbons	0.98			
		Diterpenes oxygenated	20.23			

Peak= Compounds listed in order of elution from a HP-5MS column; RI calc.=identification based on the calculated retention index (RI) utilizing a standard homologous series of n-alkanes C7 -C26 in HP-5MS UI column; Ri lit. = identification based on the comparison of mass spectra found in NIST 11.0 libraries; Relative area (%) = percentage of the area occupied by compounds in the chromatogram; RT= Retention time. The data are representative of one out of three independent experiments.

3.2. Nanoparticle Characterization

Incorporating *T. riparia* EO into PLA nanoparticles (NPs) prevented rapid EO evaporation and degradation, thereby enhancing its stability. DLS measurements indicated that NP size ranged from 221.9 to 396.5 nm. SEM and TEM images showed that the NPs were spherical, had smooth surfaces, and exhibited nanometric diameters (Figure 1).

© 2025 by the author(s). Distributed under a Creative Commons CC BY license.

Preprints.org (www.preprints.org) | NOT PEER-REVIEWED | Posted: 5 December 2025 doi:10.20944/preprints202512.0548.v1

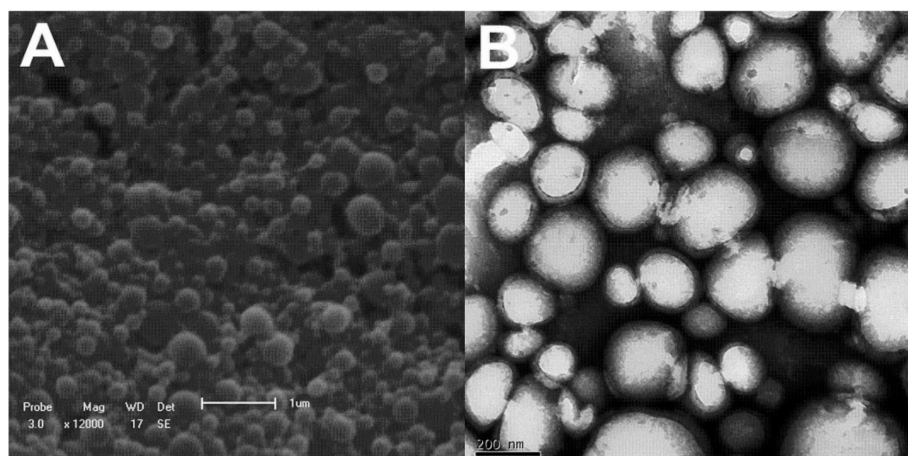

Figure 1. (**A**) Scanning electron microscopy and (B) Transmission electron microscopy images of PLA nanoparticles loaded with T. riparia essential oil. The data are representative of one out of three independent experiments.

Nanoencapsulation of aromatic molecules into capsules measuring 10–1000 nm can protect volatile compounds and significantly increase their biological activity. At the nanoscale, delivery systems may enhance passive cellular uptake, reduce mass transfer resistance, and consequently increase biological activity [39].

The surface morphology of the nanoparticles was also relevant. TEM images showed no cracks or pores on the nanocapsule surfaces. Considering that the bioactive constituents of *T. riparia* EO are highly volatile, the absence of surface fissures indicates effective protection against premature release, degradation, or interactions with environmental factors.

Nanoencapsulation is a promising strategy for controlling EO release. It prolongs antimicrobial effects, improves pharmacological efficacy, enhances water solubility, reduces toxicity, and increases patient compliance and convenience [7].

3.3. Differential Scanning Calorimetry (DSC)

DSC analysis provides insights into thermal stability by quantifying enthalpy changes associated with thermal transitions. Table 2 summarizes the DSC results. The melting temperature and melting enthalpy of blank NPs were 54.29 °C and 429.63 J/g, respectively. For NPs loaded with EO, these values decreased to 52.71 °C and 115.83 J/g. The reduction in melting enthalpy (from 429.63 to 115.83 J/g) suggests that the incorporation of EO favors controlled release.

Table 2. Melting temperatures (Tm) and melting enthalpy (ΔHm) of blank NP and NP.

Experimental condition	Tm °C	ΔHm (J/g)
Blank NP	54.29	429.63
NP	52.71	115.83

The results represent mean values for at least three separate experiments. Standard errors were less than 10% of means.

The DSC thermograms in Figure 2 show a larger endothermic peak for blank NPs. In contrast, EO-loaded NPs exhibited a smaller peak area, indicating that the EO may alter the crystalline organization of the polymer matrix, facilitating melting and consequently promoting EO release. This behavior is advantageous for controlled-release applications.

© 2025 by the author(s). Distributed under a Creative Commons CC BY license.

Preprints.org (www.preprints.org) | NOT PEER-REVIEWED | Posted: 5 December 2025 doi:10.20944/preprints202512.0548.v1

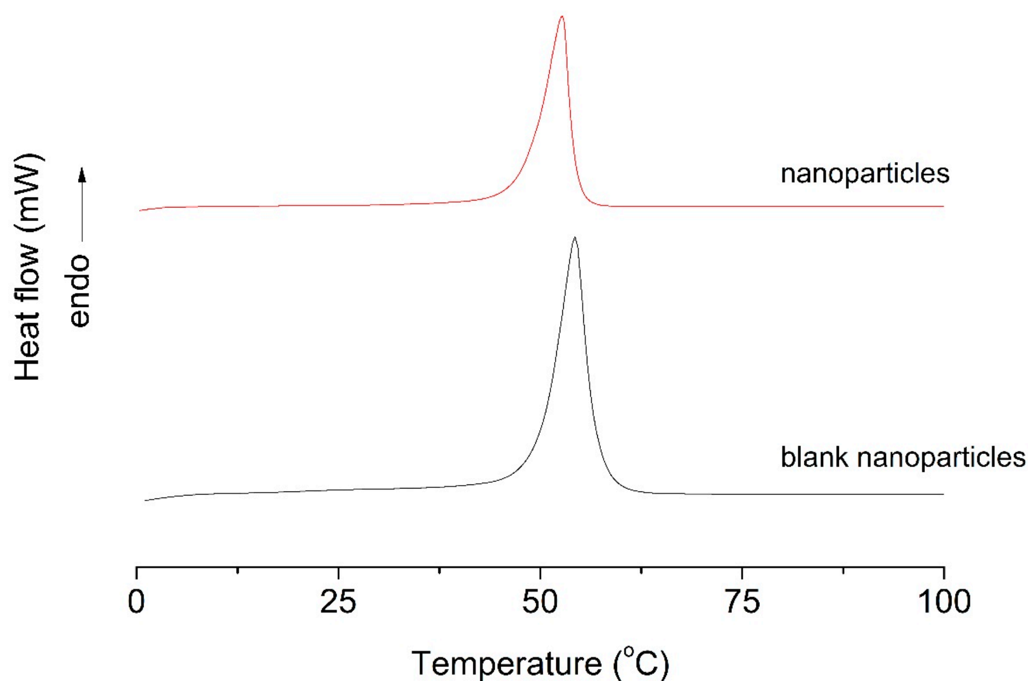

Figure 2. DSC thermograms of blank nanoparticles and nanoparticles The data are representative of one out of three independent experiments.

3.4. Encapsulation Efficiency

The amount of EO encapsulated in the nanoparticles was quantified by UV–Vis spectrophotometry at 325 nm. Encapsulation efficiency was 88.1%, indicating high EO loading and suggesting that the NPs are effective carriers [40].

Zeta potential measurements were used to assess NP stability. Zeta potential reflects surface charge, which influences dispersion stability, flocculation behavior, and interactions with negatively charged cell membranes [41,42]. The NPs exhibited a zeta potential of −23.1 mV, indicating adequate stability [43].

3.5. In Vitro Release

In vitro release profiles of free EO and NP-encapsulated EO were measured at 325 nm. Neither formulation exhibited complete release within the assay period; maximum release reached 90.0% for free EO and 25.5% for NP-encapsulated EO within 360 minutes (Figure 3). Free EO was rapidly released, whereas NP encapsulation markedly slowed the release rate. NPs maintained approximately 25.0% release after 100 minutes. The controlled-release behavior likely results from the compact network formed by poly(L-lactide) crosslinking, consistent with previous studies.

© 2025 by the author(s). Distributed under a Creative Commons CC BY license.

Preprints.org (www.preprints.org) | NOT PEER-REVIEWED | Posted: 5 December 2025 doi:10.20944/preprints202512.0548.v1

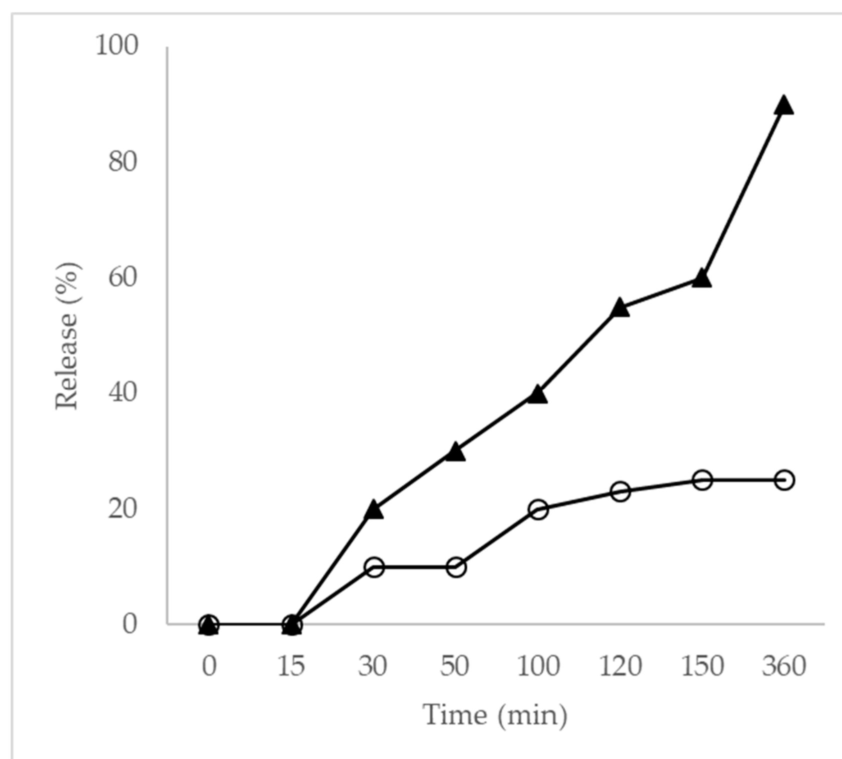

Figure 3. Release profile curve (▲) EO and (O) NP. The results represent mean values for at least three separate experiments. Standard errors were less than 10% of means.

3.6. Antibacterial Activity

The antibacterial activity of EO and NP was evaluated against *S. aureus* ATCC 29213 using broth microdilution assays (Table 3). Samples were classified as follows: MIC ≤ 0.5 mg/mL indicated strong antibacterial activity; 0.6–1.5 mg/mL indicated moderate activity; and MIC > 1.6 mg/mL indicated inactivity [44].

Table 3. Minimal inhibitory concentrations (MIC), minimal bactericidal concentrations (MBC), and 50% biofilm inhibitory concentration (BIC50) in µg/mL of EO, NP, and vancomycin against *S. aureus*.

Microorganism	**EO (µg/mL)**			**NP (µg/mL)**			**VANCO (µg/mL)**		
S. aureus	MIC	MBC	BIC_{50}	MIC	MBC	BIC_{50}	MIC	MBC	BIC_{50}
	125	250	310	250	250	330	0.4	-	9.5

The data are representative of one out of three independent experiments.

EO and NP exhibited similar antibacterial activity against both planktonic and biofilm forms of *S. aureus*, indicating that nanoencapsulation did not diminish EO activity. However, enhanced antibacterial activity after encapsulation would have been desirable.

The antibiofilm effects of EO and NP were compared with vancomycin. BIC_{50} values were 310 µg/mL for EO and 330 µg/mL for NP.

Biofilm morphology after treatment is shown in Figure 4. SEM analysis revealed that untreated cells (A) appeared spherical, dense, and surrounded by abundant extracellular matrix. EO-treated biofilm (B) showed reduced extracellular matrix, altered cell morphology, and fewer cells. NP-treated biofilm (C) also exhibited decreased cell numbers and notable alterations in the cell wall and membrane, suggesting irreversible membrane damage, as previously described by Kang et al. [45].

© 2025 by the author(s). Distributed under a Creative Commons CC BY license.

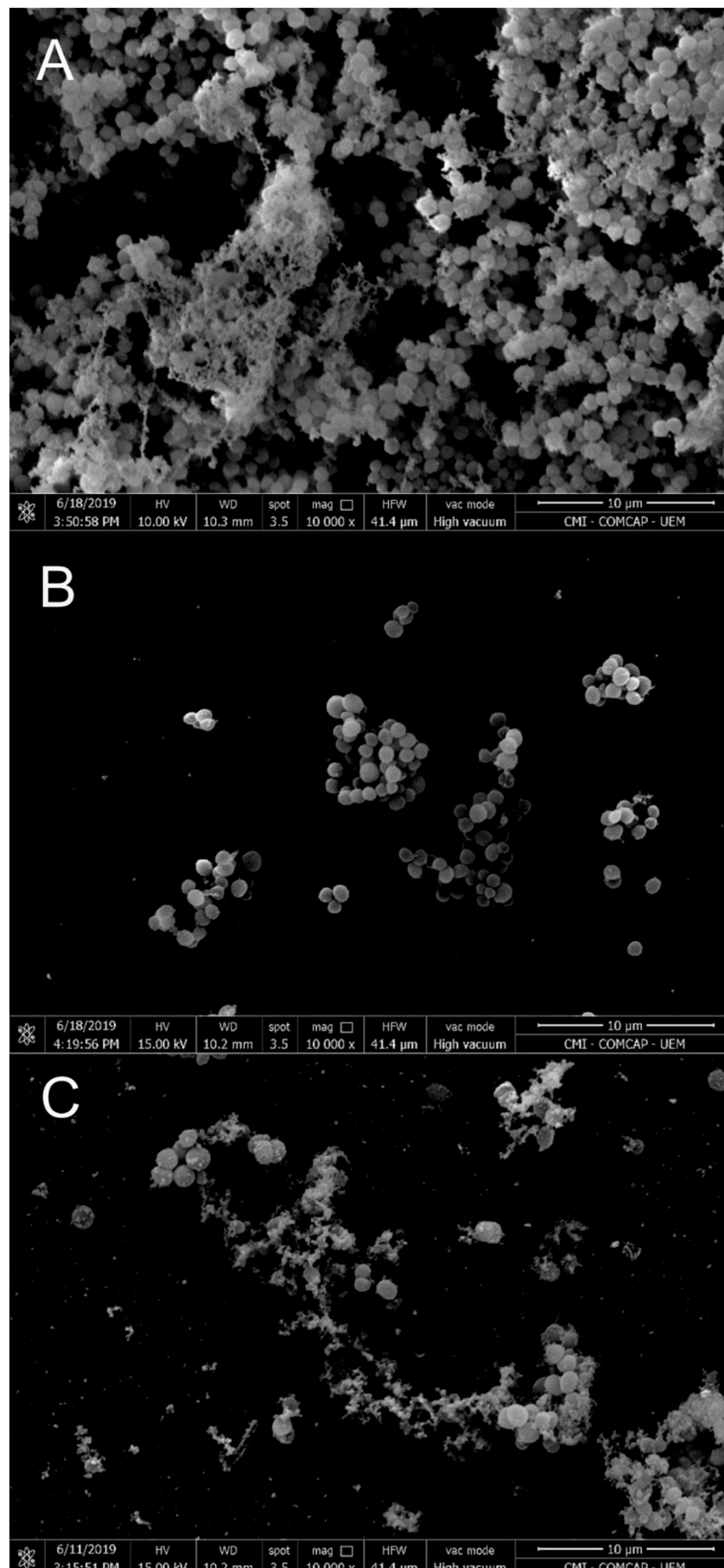

Figure 4. Scanning electron microscopy. (**A**) *S. aureus* biofilm control (untreated); (**B**) Biofilm treated with a subinhibitory concentration of EO; (**C**) Biofilm treated with a subinhibitory concentration of NP. Magnification: 10,000×. Scale bars: 10 µm. The data are representative of one out of three independent experiments.

Kwieciński et al. [46] reported that treatment with 1% tea tree EO completely eradicated *S. aureus* biofilm, causing not only bacterial death but also matrix disruption and biofilm detachment from surfaces.

© 2025 by the author(s). Distributed under a Creative Commons CC BY license.

Preprints.org (www.preprints.org) | NOT PEER-REVIEWED | Posted: 5 December 2025

doi:10.20944/preprints202512.0548.v1

3.7. Cytotoxicity Assay

Although EOs are widely used as antimicrobial agents, their clinical effectiveness depends on the relationship between effective in vitro concentrations and the concentrations achievable at the site of action. Cytotoxicity varies depending on EO constituents, and several attempts have been made to correlate in vitro and in vivo toxicities. Antimicrobial agents must selectively target microorganisms, exhibit minimal effects on host cells, and avoid interfering with normal physiological pathways. According to the U.S. National Cancer Institute (NCI), crude extracts with $IC_{50} \leq 20$ μg/mL are considered cytotoxic [47–49].

Table 4 summarizes the cytotoxicity results. IC_{50} values for NP and EO were 533.96 μg/mL and <125 μg/mL, respectively. NPs were less cytotoxic to VERO cells than free EO, demonstrating that encapsulation reduced EO toxicity. This finding supports nanoencapsulation as an effective approach to modulate release profiles while minimizing toxicity [50].

Table 4. Cytotoxicity assay of free and nanoencapsulated *T. riparia* EO on VERO cells.

Drug	IC_{50} (μg/mL)
EO	<125
NP	533.96

The data are representative of one out of three independent experiments.

5. Conclusions

Tetradenia riparia essential oil displayed a consistent chemical profile rich in oxygenated monoterpenes and sesquiterpenes, which supports its biological potential. PLA nanoencapsulation successfully stabilized the EO, provided high encapsulation efficiency, and enabled controlled and sustained release. Although antibacterial activity against *Staphylococcus aureus* was not enhanced, nanoencapsulation preserved the EO's efficacy while significantly reducing cytotoxicity. These findings demonstrate that PLA nanoparticles are an effective delivery system for optimizing the stability and safety of *T. riparia* EO, reinforcing their suitability for future pharmacological development.

Supplementary Materials: The following supporting information can be downloaded at the website of this paper posted on Preprints.org.

Author Contributions: Conceptualization, data curation, formal analysis investigation, R.Y.M. and E.H.E.; contributions in methodology, J.W.M. and C.V.N.; assisted in methodology P.F.R. and F.V.L.; contributed in methodology, O.H G. and Z.C G.; conceptualization, funding acquisition, writing review & editing, E.H.E. and B.P.D.F. All these authors have substantial contributions to the final manuscript and have approved this submission. All authors are aware of the order of authorship and that no further change in authorship will be performed after submission, except for those previously authorized by the editor-in-chief.

Acknowledgments: This study was supported by Conselho Nacional de Desenvolvimento Científico e Tecnológico (CNPq), Financiadora de Estudos e Projetos (FINEP), Capacitação e Aperfeiçoamento de Pessoal de Nível Superior, (Capes), Fundação Araucária, and Programa de Pós-graduação em Ciências Farmacêuticas da Universidade Estadual de Maringá; Complexo de Centrais de Apoio à Pesquisa (COMCAP/UEM).

Conflicts of Interest: The authors declare no conflicts of interest.

Abbreviations

EO	Essential oils
NP	Nanoparticles
PLA	Poly (L-lactide)
DLS	Dynamic light scattering
SEM	Scanning electron microscopy.

© 2025 by the author(s). Distributed under a Creative Commons CC BY license.

Preprints.org (www.preprints.org) | NOT PEER-REVIEWED | Posted: 5 December 2025
doi:10.20944/preprints202512.0548.v1

TEM	Transmission electron microscopy
DSC	Differential scanning calorimetry
MHA	Mueller Hinton Agar
MHB	Mueller Hinton Broth
CFU	Colony forming unit
MIC	Minimum inhibitory concentration
MBC	Minimum bactericidal concentration
PBS	Phosphate-buffered saline
TSB	Tryptic soy broth
MTT	Dimethylthiazol-2-yl-2,5-diphenyl tetrazolium bromide
DMSO	Dimethyl sulfoxide
BIC_{50}	50% biofilm inhibitory concentration
OD	Optical density
DMEM	Dulbecco's Modified Eagle's Medium
IC_{50}	50% inhibitory concentrations

References

1. Goldmann, O.; Medina, E. *Staphylococcus aureus* strategies to evade the host acquired immune responde. *Int. J. Med. Microb.* **2018,** 308, 625-630. DOI: 10.1016/j.ijmm.2017.09.013
2. Albano, M.; Crulhas, B.P.; Alves, F.C.B.; Pereira, A.F.M.; Andrade, B.F.M.T.; Barbosa, LN.; Furlanetto, A.; Lyra, L.P.S.; Rall, V.L.M.; Fernandes Júnior, A. Antibacterial and anti-biofilm activities of cinnamaldehyde against *S. epidermidis*. *Microb. Pathog*. **2019,** 126, 231-238. DOI: 10.1016/j.micpath.2018.11.009
3. Forier, K.; Raemdonck, K.; De Smedt, S.C.; Demeester, J.; Coenye, T.; Braeckmans, K. Lipid and polymer nanoparticles for drug delivery to bacterial biofilms. *J. Control. Release* **2014,** 190, 607-623. DOI: 10.1016/j.jconrel.2014.03.055
4. Soares, V.B.; Morais, S.M.; Fontenelle, R.O.S.; Queiroz, V.A.; Vila-Nova, N.S.; Pereira, C.M.C.; Brito, E.S.; Neto, M.A.; Brito, E.H.S.; Cavalcante, C.S.P.; Castelo-Branco, D.S.C.M.; Rocha, M.F.G. 2012. Antifungal activity, toxicity and chemical composition of the essential oil of *Coriandrum sativum* L. fruits. *Molecules* **2012,** 17, 8439-8448. DOI: 10.1111/j.1365-2672.2007.03707.x
5. Raut, J.S.; Karuppayil, S.M. A status review on the medicinal properties of essential oil. *Ind. Crops Prod.* **2014,** 62, 250-264. https://doi.org/10016/j.indcrop.2014.05.055
6. Jamalian, A.; Shams-Ghahfarokhi, M.; Jaimand, K.; Pashootan, N.; Amani, A.; Razzaghi-Abyyaneh, M. Chemical composition and antifungal activity of *Matricaria recutita* flower essential oil against medically important dermatophytes and soil-borne pathogens. *J. Mycol. Med.* **2012**, 308-315. DOI: 10.1016/j.mycmed.2012.09.003
7. São-Pedro, A.; Espirito-Santo, I.; Silva, V.C. Albuquereque, E. The use of nanotechnology as an approach for essential oil-based formulations with antimicrobial activity. Microbial Pathogens (A. Mendez-Vilas. Ed.). 2013 1, 1364-1374. https://doi.org/10.1590/S1984-82502016000300001
8. Gairola, S.; Yougasphree Naidoo, Y.; Bhatt, A.; Nicholas, A. An investigation of the foliar trichomes of *Tetradenia riparia* (Hochst.) Codd [Lamiaceae]: An important medicinal plant of Southern Africa. *Flora* **2009,** 204, 325-330. DOI: 10.1016/j.flora.2008.04.002
9. Gazim, Z.C.; Rodrigues, F.; Amorim, A.C.L.; Rezende, C.M.; Sokovic, C.M.; Tesevic, V.; Vuchovic, I., Krstic, G., Cortez, L.E.R.; Colauto, N.B.; Linde, G.A.; Cortez, D.A.G. New natural diterpene-type abietane from *Tetradenia riparia* essential oil with cytotoxic and antioxidant activities. *Molecules* **2014,** 19, 514-524. DOI: 10.3390/molecules19010514
10. Gazim, Z.C.; Amorim, A.C.; Hovell, A.M.; Rezende, C.M.; Nascimento, A.; Ferreira, G.A.; Cortez, D.A.G. Seasonal variation, chemical composition, analgesic and antimicrobial activities of the essential oil from leaves of *Tetradenia riparia* (Hochst.) Codd in Southern Brazil. *Molecules* **2010,** 15, 5509-5524. DOI: 10.3390/molecules15085509
11. Oliveira, P.F.; Alves, J.M.; Damasceno, J.L.; Oliveira, R.A.M.; Dias, H.J.; Crotti, A.E.M.; Tavares, D.C. Cytotoxicity screening of essential oils in cancer cell lines. *Rev. Bras. Farmacogn.* **2015,** 25, 183-188. https://doi.org/10.1016/j.bjp.2015.02.009

© 2025 by the author(s). Distributed under a Creative Commons CC BY license.

Preprints.org (www.preprints.org) | NOT PEER-REVIEWED | Posted: 5 December 2025 doi:10.20944/preprints202512.0548.v1

12. Njau, E.A.; Alcorn, J.; Buza, J.; Chirino-Trejo, M.; Ndakidemi, P. Antimicrobial activity of *Tetradenia riparia* (Hochst.) *Lamiaceae*, a medicinal plant from Tanzania. *Eur. J. Med. Plants* **2014,** 4, 1462-DOI: 10.9734/EJMP/2014/11370
13. Oliveira, E.F.; Paula, H.C.B.; Paula, R.C.M. Alginate/cashew gum nanoparticles for essential oil encapsulation. *Coll Surf B* **2014,** 113, 146-151. DOI: 10.1016/j.colsurfb.2013.08.038
14. Gazim, Z.C.; Demarchi, I.G.; Lonardoni, M.V.C.; Amorim, A.C.L.; Hovell, A.M.C.; Rezende, C.M.; Ferreira, C.M.; Lima, E.L.; Cosmo, F.A.; Cortez, D.A.G. Acaricidal activity of the essential oil from *Tetradenia riparia* (Lamiaceae) on the cattle tick *Rhipicephalus* (Boophilus) *mocroplus* (Acari: Ixodidae). *Exp. Parasitol.* **2011,** 29, 175-178. DOI: 10.1016/j.exppara.2011.06.011
15. Barwall, I.; Sood, A.; Sharma, M.; Singh, B.; Yadav, S.C. 2013. Development of stevioside Pluronic F-68 copolymer based PLA-nanoparticles as an antidiabetic nanomedicine. *Coll Surf B* **2013**, 101, 510-516. DOI: 10.1016/j.colsurfb.2012.07.005
16. Guimarães, G. P. Estabilidade de Medicamentos Sintéticos: Visão Geral da nova Diretriz da Anvisa. 2020.
17. Clinical and Laboratory Standards Institute: Methods for dilution antimicrobial susceptibility test for bacteria that grow aerobically. Approved standard, 9th ed. M07-A9, CLSI, **2012**, Wayne, PA
18. Schillaci, D.; Arizza, V.; Dayton, T.; Camarda, L.; Stefano, V.D. In vitro anti-biofilm activity of *Boswellia* spp. oleogum resin essential oils. *Lett. Appl. Microbiol.* **2008,** 47, 433–438. doi: 10.1111/j.1472-765X.2008.02469.x.
19. Tangarife-Castaño, V.; Roa-Linares, V.; Betancur-Galvis, L.A.; Garcia, D.C., Stashenko, E.; Mesa-Arango, A.C. Antifungal activity of Verbenaceae and Labitae families essential oils. *Pharmacologyonline* **2011,** 1,, 133-145. DOI: 10.1080/10412905.2013.82067
20. Smadja, J.; Rondeau, P.; Sing, A.S.C. Volatile constituents of five *Citrus petitgrain* essential oils from Reunion. *Flavour Fragr. J.* **2005**, *20*(4), 399-402. https://doi.org/10.1002/ffj.1438.
21. Pavlovic, M.; Kovacevic, N.; Tzakou, O.; Couladis, M. Essential oil composition of *Anthemis triumfetti* (L.) DC. *Flavour Fragr. J.* **2006**, *21*(2), 297-299. https://doi.org/10.1002/ffj.1592.
22. Pérez, R.A.; Navarro, T.; de Lorenzo, C. HS-SPME analysis of the volatile compounds from spices as a source of flavour in 'Campo Real' table olive preparations. *Flavour Fragr. J.* **2007**, *22*(4), 265-273. https://doi.org/10.1002/ffj.1791.
23. Petrakis, P.V.; Roussis, V.; Papadimitriou, D.; Vagias, C.; Tsitsimpikou, C. The effect of terpenoid extracts from 15 pine species on the feeding behavioural sequence of the late instars of the pine processionary caterpillar *Thaumetopoea pityocampa*. *Behav. Processes.* **2005**, *69*(3), 303-322. https://doi.org/10.1016/j.beproc.2004.12.008.
24. Zhao, C.X.; Liang, Y.Z.; Fang, H.Z.; Li, X.-N. Temperature-programmed retention indices for gas chromatography-mass spectroscopy analysis of plant essential oils. *J. Chromatogr. A.* **2005**, *1096*(1-2), 76-85. https://doi.org/10.1016/j.chroma.2005.09.067.
25. Baranauskiene, R.; Venskutonis, P.R.; Viskelis, P.; Dambrauskiene, E. Influence of nitrogen fertilizers on the yield and composition of thyme (*Thymus vulgaris*). *J. Agric. Food Chem.* **2003**, *51*(26), 7751-7758. https://doi.org/10.1021/jf0303316.
26. Zhao, C.X.; Li, X.N.; Liang, Y.Z.; Fang, H.Z.; Huang, L.F.; Guo, F.Q. Comparative analysis of chemical components of essential oils from different samples of *Rhododendron* with the help of chemometrics methods. *Chemom. Intell. Lab. Syst.* **2006**, *82*(1-2), 218-228. https://doi.org/10.1016/j.chemolab.2005.08.008.
27. Hazzit, M.; Baaliouamer, A.; Faleiro, M.L.; Miguel, M.G. Composition of the Essential Oils of *Thymus* and *Origanum* Species from Algeria and Their Antioxidant and Antimicrobial Activities. *J. Agric. Food Chem.* **2006**, *54*(17), 6314-6321. https://doi.org/10.1021/jf0606104.
28. Kukic, J.; Petrovic, S.; Pavlovic, M.; Couladis, M.; Tzakou, O.; Niketic, M. Composition of essential oil of *Stachys alpina* L. ssp dinarica Murb. *Flavour Fragr. J.* **2006**, *21*(3), 539-542. https://doi.org/10.1002/ffj.1684.
29. Siani, A.C.; Garrido, I.S.; Monteiro, S.S.; Carvalho, E.S.; Ramos, M.F.S. *Protium icicariba* as a source of volatile essences. *Biochem. Syst. Ecol.* **2004**, *32*(5), 477-489. https://doi.org/10.1016/j.bse.2003.11.003.
30. Siani, A.C.; Ramos, M.F.S.; Menezes-de-Lima, O., Jr.; Ribeiro-dos Santos, R.; Fernandez-Ferreira, E.; Soares, R.O.A.; Rosas, E.C.; Susunaga, G.S.; Guimarães, A.C.; Zoghbi, M.G.B.; Henriques, M.G.M.O. Evaluation of anti-inflammatory-related activity of essential oils from the leaves and resin of species of *Protium*. *J. Ethnopharmacol.* **1999**, *66*(1), 57-69. https://doi.org/10.1016/S0378-8741(98)00148-2.

© 2025 by the author(s). Distributed under a Creative Commons CC BY license.

Preprints.org (www.preprints.org) | NOT PEER-REVIEWED | Posted: 5 December 2025 doi:10.20944/preprints202512.0548.v1

31. Chorianopoulos, N.; Evergets, E.; Mallouchos, A.; Kalpoutzakis, E.; Nychas, G.J.; Haroutounian, S.A. Characterization of the essential oil volatiles of *Satureja thymbra* and *Satureja parnassica*: Influence of harvesting time and antimicrobial activity. *J. Agric. Food Chem.* **2006**, *54*(8), 3139-3145. https://doi.org/10.1021/jf053183n.
32. Weyerstahl, P.; Marschall, H.; Splittgerber, U.; Wolf, D.; Surburg, H. Constituents of Haitian vetiver oil. *Flavour Fragr. J.* **2000**, *15*(6), 395-412. https://doi.org/10.1002/1099-1026(200011/12)15:6<395::AID-FFJ930>3.0.CO;2-9.
33. Alonzo, G.; Bosco, S.F.D.; Palazzolo, E.; Saiano, F.; Tusa, N. Citrus somatic hybrid leaf essential oil. *Flavour Fragr. J.* **2000**, *15*(4), 258-262. https://doi.org/10.1002/1099-1026(200007/08)15:4
34. Roussis V.; Tsoukatou M.; Petrakis P.V.; Chinou I.B.; Skoula M.; Harborne J.B. Volatile Constituents of Four *Helichrysum* Species Growing in Greece. *Biochem. Syst. Ecol.* **2000**, *28*, 163–175. https://doi.org/10.1016/S0305-1978(99)00046-0.
35. Monsef-Esfahani, H.R.; Miri, A.; Amini, M.; Amanzadeh, Y.; Hadjiakhoondi, A.; Hajiaghaee, R.; Ajani, Y. Seasonal variations in the chemical composition, antioxidant activity and total phenolic content of *Teucrium persicum* Boiss. essential oils. *Res. J. Biol. Sci.* **2010**, *5*(7), 492-498. https://doi.org/10.3923/rjbsci.2010.492.498.
36. Vujisic, L.; Vuckovic, I.; Tesevic, V.; Dokovic, D.; Ristic, M.S.; Janackovic, P.; Milosavljevic, S. Comparative examination of the essential oils of *Anthemis ruthenica* and *A. arvensis* wild-growing in Serbia. *Flavour Fragr. J.* **2006**, *21*(3), 458-461. https://doi.org/10.1002/ffj.1681.
37. Flamini, G.; Tebano, M.; Cioni, P.L.; Bagci, Y.; Dural, H.; Ertugrul, K.; Uysal, T.; Savran, A. A multivariate statistical approach to Centaurea classification using essential oil composition data of some species from Turkey. *Pl. Syst. Evol.* **2006**, *261*(1-4), 217-228. https://doi.org/10.1007/s00606-006-0448-3.
38. Sena, J.D.S.; Rodrigues, S.A.; Sakumoto, K.; Inumaro, R.S.; González-Maldonado, P.; Mendez-Scolari, E.; Gazim, Z.C. Antioxidant activity, antiproliferative activity, antiviral activity, NO production inhibition, and chemical composition of essential oils and crude extracts of leaves, flower buds, and stems of *Tetradenia riparia*. *Pharmaceuticals.* **2024**, *17*(7), 888. https://doi.org/10.3390/ph17070888
39. Ali, H.; Al-Khalifa, A. R.;Aouf, A.; Boukhebti, H.; Farouk, A. Effect of nanoencapsulation on volatile constituents, and antioxidant and anticancer activities of Algerian *Origanum glandulosum* Desf. essential oil. *Sci. Rep*. **2020,** 10(1), 2812
40. Feng-Lian Y, Zue-Gang L, Zhu F. Structural characterization of nanoparticles loaded with garlic essential oil and their insecticidal activity against *Tribolium castaneum* (Herbst) (Coleoptera: Tenebrionidae). *J. Agric. Food Chem*. **2009**, 10156:10162-57. DOI: 10.1021/jf9023118.
41. Chen, F.; Shi, Z.; Neoh, K.G.; Kang, E.T. Antioxidant and antibacterial activities of Eugenol and Carvacrol-grafted chitosan nanoparticles. *Biotechnol. Bioeng*. **2009**, 104, 30-39. DOI: 10.1002/bit.22363
42. Schaffazick, S. R., Guterres, S. S., Freitas, L. L., Pohlmann, A. R., 2003. Caracterização e estabilidade físico-química de sistemas poliméricos nanoparticulados para administração de fármacos. *Quím. Nova,* **2003**, 26, 726-737. https://doi.org/10.1590/S0100-40422003000500017
43. Anitha, A.; Deepagan, V.G.; Divya Rani, V.V.; Deepthy Menon, S.V.N.; Jayakumar, R. Preparation, characterization, in vitro drug release and biological studies of curcumin loaded dextran sulphate-chitosan nanoparticles. *Carbohydr. Polym*. **2011,** 84, 1158-1164. DOI: 10.1016/j.carbpol.2011.01.005
44. Duarte, M.C.T.; Figueira, G.M.; Sartoratto, A.; Rehder, V.L.G.; Delamarmelina, C.. Anti-Candida activity of Brazilian medicinal plants. *J. Ethnopharmacol*. **2005**, 97, 305-311. DOI: 10.1016/j.jep.2004.11.016
45. Kang, J.; Jin, W.; Wang, J.; Sun, Y.; Wu, X.; Liu, L. Antibacterial and anti-biofilm activities of peppermint essential oil against *S. aureus*. LWT – *Food Science and Technology,* **2019,** 101, 639-645.
46. Kwiecinski, J.; Eick, S.; Wojcik, K. Effects of tea tree (*Melaleuca alternifolia*) oil on in biofilms. ***Int. J. Antimicrob. Agents***, **2009**, 33, 343-347.
47. Reichiling, J.; Schnitzler, P.; Sushke, U.; Saller, R. Essential oils of aromatic plants with antibacterial, antifungal, antiviral and cytotoxic properties – an overview. *Forsch. Komplementmed.* **2009**, 16, 79-90. DOI: 10.1159/000207196
48. Sifi, I.; Dzoyem, J.P.; Quinten, M.; Yousfi, M.; Mcgaw, L.J.; Eloff, J.N. Antimycobacterial, antioxidant and cytotoxic activities of essential oil of gall of *Pistacia atlantica* desf. from Algeria. *Afr. J. Tradit. Complement Altern. Med.* **2015**, 12, 150-155. DOI: 10.4314/ajtcam.v12i3.2843

© 2025 by the author(s). Distributed under a Creative Commons CC BY license.

Preprints.org (www.preprints.org) | NOT PEER-REVIEWED | Posted: 5 December 2025 doi:10.20944/preprints202512.0548.v1

49. Vijayarathna, S.; Sasudharan, S. Cytotoxicity of methanol extracts of *Elaeis guineensis* on MCF-7 and VERO cell lines. *Asian Pac. J. of Trop. Biomed.* **2012**, 2, 826-829. DOI: 10.1016/S2221-1691(12)60237-8
50. Bilia, A.R.; Guccione, C.; Isacchi, B.; Righeschi, C.; Firenzuolo, F.; Bergonzi, C. Essential oils loaded in nanosystem: A developing strategy for a successful therapeutic approach. *Evid. Based Complement. Alternat. Med*. **2014,** 6, 51-59. DOI: 10.1155/2014/651593

Disclaimer/Publisher's Note: The statements, opinions and data contained in all publications are solely those of the individual author(s) and contributor(s) and not of MDPI and/or the editor(s). MDPI and/or the editor(s) disclaim responsibility for any injury to people or property resulting from any ideas, methods, instructions or products referred to in the content.

© 2025 by the author(s). Distributed under a Creative Commons CC BY license.